Temperature-Dependent Macromodels of Digital Device

TEMPERATURE-DEPENDENT MACROMODELS OF DIGITAL DEVICES

I. S. Stievano, I. A. Maio, F. G. Canavero
Dip. Elettronica - Politecnico di Torino, 10129 Torino, Italy
(Principal contact: stievano@polito.it)

Abstract: This paper addresses the development of a temperature-dependent parametric macromodel for the output ports of a digital IC. The model parameters are estimated from port transient voltage and current waveforms by means of a simple and efficient procedure. The obtained models are implemented as SPICE subcircuits. They perform at an accuracy and efficiency level suitable for system-level SI and EMC simulations.

1. Introduction

Nowadays, the design of high performance digital circuits requires the assessment of Signal Integrity (SI) and ElectoMagnetic Compatibility (EMC) effects at the early stage of the design process. Such an assessment is mainly achieved by the numerical simulation of signals propagating on-board or on-chip interconnect structures. In these simulations, a key role is played by the numerical models available for digital Integrated Circuits (ICs), that act as receivers or signal pattern generators loading the interconnects. The sought models must be efficient enough to handle the complexity of actual simulation problems and include high-order effects needed for accurate predictions.

Since we are interested in the external behavior of ICs, the best way to build IC models matching the above requirements is via the development of behavioral models or macromodels. IC macromodels, therefore are relations between the voltages and the currents of the IC ports for a known internal logic activity.

The first and most common resource available to accomplish such a task is the description of IC ports by means of simplified equivalent circuits, because equivalents allow physical insight and facilitate the implementation of models. An important example of the equivalent circuit approach to behavioral modeling is the widely adopted Input/output Buffer Information Specification (IBIS) [1], that has given rise to a large set of dedicated model libraries for the Electronic Design Automation tools. The equivalent circuit approach, however, has also some inherent limitations. Mainly, the estimation of model parameters is best performed by virtual measurements carried on transistor-level models of the IC. In addition, the circuit structure defining the model decides *a-priori* the physical effects to be considered, leaving no possibilities to reproduce other effects inherent to a specific device.

A second possible resource is the use of parametric models and input-output system identification methods [2, 3, 4] to approximate the IC port constitutive relations. In this approach, the parameters of a suitable model are estimated from the voltage and current waveforms measured or simulated at the device ports. The parametric approach to behavioral modeling has interesting advantages, that makes it a useful complement to the more traditional equivalent circuit approach. It automatically takes into account any physical effects significantly influencing voltages and currents of the IC ports and yields models that perform at a very good accuracy level with relatively high efficiency. Also the accuracy level of the models turns out to be weakly sensitive to the load they drive.

For IC ports, the generic macromodel is a constitutive relation of the form

$$i(t) = F(v(t), w(t); T; P_1; P_2, \ldots) \qquad (1)$$

where $i(t)$ and $v(t)$ are the port current and voltage, respectively, F is a nonlinear dynamic operator, $w(t)$ is an extra input needed to specify the port transitions, T is the temperature and $P_1, P_2, \ldots$ are other possible extra variables affecting the external behavior of the port, like the power supply voltages.

2. Output port macromodel

The aim of this Section is to briefly introduce the parametric macromodeling technique for the output ports of digital ICs. The parametric model that is going to be presented was developed and described in [3]. It concerns the functional part of the devices, and assumes constant all other parameters influencing their behavior. Here, we mainly focus on the definition of such parametric model representation and on the estimation of its parameters from port transient waveforms.

The model is of discrete-time type and involves the sam-

ples of the port electric voltage $v(k) = v(kt_s)$ and current $i(k) = i(kt_s)$, where t_s is the sampling time used to sample the time axis. For output ports, the following model representation is exploited

$$i(k) = w_1(k)i_1(k) + w_2(k)i_2(k) \quad (2)$$

where w_1 and w_2 are time varying weight sequences playing the role of the extra input $w(t)$ in (1) and accounting for state switchings in (2). Submodels i_1 and i_2 are parametric representations defined by Radial Basis Function (RBF) expansions and approximating both the nonlinear static and dynamic $i - v$ port behavior in the High and in the Low fixed logic states, respectively.

RBF parametric models are suitable for the characterization of the external behavior of many nonlinear dynamic systems [5]. They approximate the input-output system behavior, *i.e.,* for the problem at hand the $i - v$ port relation, through a finite weighted sum of scalar basis functions (*e.g.,* Gaussian) with a suitable width and proper position. In particular, the submodels $i_n,\ n = 1, 2$ of (2) are defined by

$$i_n(k) = \sum_j \alpha_{nj}\phi_j(\boldsymbol{x}_n(k)) \quad (3)$$

where $\boldsymbol{x}_n$ is the regressor vector

$$\boldsymbol{x}_n(k) = [i_n(k-1), \ldots, i_n(k-r), v(k), \ldots, v(k-r)]^T$$

collecting the present sample of the port voltage v and past r samples of v and i, r being the dynamic order of the model. ϕ_j is the j-th Gaussian basis function

$$\phi_j(\boldsymbol{x}_n(k)) = \exp\{-||\boldsymbol{x}_n(k) - \boldsymbol{c}_{nj}||^2/(2\beta_n^2)\}$$

defined by a position (center $\boldsymbol{c}_{nj}$) in the space of the regressor vector $\boldsymbol{x}_n$ and by a width (spreading parameter β_n). The complete set of unknown parameters defining the model are the linear parameters $\boldsymbol{\alpha}_n = [\alpha_1, \alpha_2, \ldots]^T$ and the nonlinear parameters, *i.e.,* the center and the spreading of each basis function. The above time-variant two-piece model arises systematically from the property of output port structures and of RBFs and inherits most of strengths of RBF parametric models in approximating nonlinear dynamic systems.

The parameters of submodels i_n are computed from a set of transient voltage and current waveforms (named *identification signals*) by means of the application of estimation algorithms matching the model response to the port reference response [6, 7]. The identification signals are obtained by forcing the port in the High and in the Low logic state, respectively, and by recording the port current response to a multilevel voltage signal applied to the output of the port and spanning the range of operating voltages. Then, the weight coefficients w_1 and w_2 are obtained from a set of switching experiments by linear inversion of equation (2). In these experiments the port is driven to produce complete state switchings for two different load conditions and the port voltage and current waveforms are recorded. Finally, as the last step of the modeling process, the estimated output port model is implemented as a SPICE subcircuit in order to allow the use of such model for circuit simulation. This is done by converting the discrete-time model (2) into a continuous-time state-space representation and by synthesizing it into an equivalent circuit.

A more detailed discussion of the systematic derivation of model (2) together with guidelines for the estimation of its parameters and the implementation of the model in a circuit simulation environment can be found in [3], where the modeling approach has already been applied to commercial devices defined by transistor-level models [3]. Besides, it has been demonstrated that such modeling technique is equally applicable to the characterization of real devices from direct measurements taken on the external pins of the device [4].

3. Inclusion of temperature dependence

In this Section, the model representation defined by (2) is suitably modified to include the extra dependence on the temperature variable T. For typical output ports, the temperature has a weak influence on the whole dynamic port behavior, even for large variations of T. As an example, Fig. 1 shows the set of responses of a commercial high-speed driver connected to a transmission line load. The responses are computed via SPICE-type simulations of a detailed transistor-level model of the driver, for different values of T in the range $[-10, 100]\ ^\circ C$.

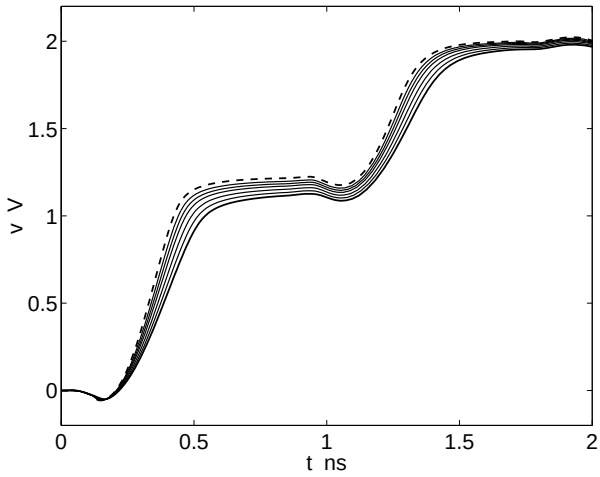

Figure 1: Example of the output port voltage response $v(t)$ of a commercial high-speed IBM CMOS driver feeding a 12 cm long transmission line. The driver performs a Low-to-High transition. The different curves refer to various operating temperatures, *i.e.,* $T = -10\,^\circ C$ (dashed thick line), $T = 100\,^\circ C$ (solid tick line) and $T = 10, 25, 40, 60, 80\,^\circ C$ (solid thin lines).

The regular behavior highlighted in Fig. 1 suggests to look for a model representation defined by

$$i(k;T) = w_1(k;T)i_1(k;T) + w_2(k;T)i_2(k;T) \quad (4)$$

where both the weight coefficients w_1 and w_2 and the RBF submodels i_1 and i_2 depend on the extra input T.

Besides, since the submodels defined by (3) are weakly sensitive to the position of centers and spreading parameters [6, 7], the temperature dependence of submodels $i_n(k;T)$ can be confined to the linear parameters $\boldsymbol{\alpha}_n$. Therefore, for the RBF submodels, this means to estimate the complete set of parameters from the transient identification curves recorded at a nominal temperature value and to obtain the parameters for other possible temperature values by re-estimating the linear parameters only. It is ought to remark that, when the centers and the spreading parameters are fixed, the estimation of the linear parameters $\boldsymbol{\alpha}_n$ can be easily done by solving a standard linear least square problem as suggested in [6].

In order to derive dependency of $\boldsymbol{\alpha}_n$ from T, we estimated the linear parameters of submodels $i_n(k)$ for several transistor-level models of commercial drivers and for different temperature values. As an example, Fig. 2 shows the entries of the linear parameter vector $\boldsymbol{\alpha}_1$ computed at $T = 10, 25, 40, 60, 80\,^{\circ}C$ for a common driver. In this example, the linear parameters are obtained by assuming constant the centers and the spreading parameter estimated at $T = 40\,^{\circ}C$.

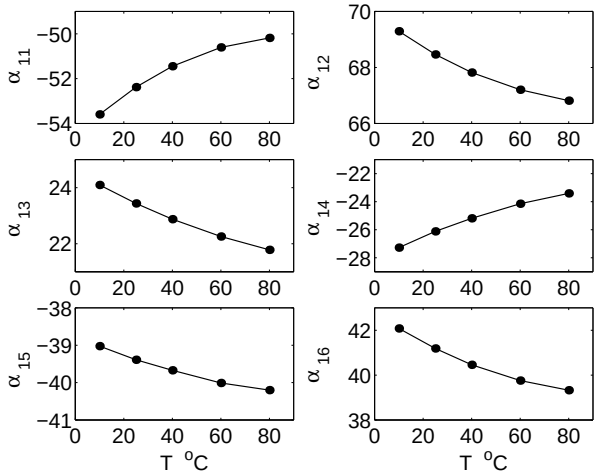

Figure 2: Example of dependency of the linear parameters $\boldsymbol{\alpha}_1$ from temperature. Dots indicate the computed values for $T = 10, 25, 40, 60, 80\,^{\circ}C$.

The curves of Fig. 2 show that a linear or a piecewise linear function can be an accurate approximation of $\boldsymbol{\alpha}_n(T)$, *i.e.,* for any T_1, T_2 and $T \in [T_1, T_2]$

$$\boldsymbol{\alpha}_n(T) \approx \bar{\boldsymbol{\alpha}}_n(T) = \left(\tfrac{T-T_2}{T_1-T_2}\right) \boldsymbol{\alpha}_n|_{T_1} + \left(\tfrac{T-T_1}{T_2-T_1}\right) \boldsymbol{\alpha}_n|_{T_2} \tag{5}$$

where $\boldsymbol{\alpha}_n|_{T_1}$ and $\boldsymbol{\alpha}_n|_{T_2}$ are the linear parameters of (2) computed at $T = T_1$ and $T = T_2$, respectively. It is ought to remark that submodels defined by $\bar{\boldsymbol{\alpha}}_n(T)$ are monotonous functions of T as those defined by the exact $\boldsymbol{\alpha}_n(T)$.

In a similar way, the relation defining the weight coefficients $w_n(k;T)$ can be represented by

$$w_n(k;T) \approx \bar{w}_n(k;T) = \left(\tfrac{T-T_2}{T_1-T_2}\right) w_n(k)|_{T_1} + \left(\tfrac{T-T_1}{T_2-T_1}\right) w_n(k)|_{T_2} \tag{6}$$

where $w_n(k)|_{T_1}$ and $w_n(k)|_{T_2}$ are the weight coefficients of (2) computed at $T = T_1$ and $T = T_2$, respectively.

The accuracy required in common simulation problems can be easily achieved by two-piece linear representations $\bar{\boldsymbol{\alpha}}_n(T)$ and $\bar{w}_n(k;T)$ defined by three temperature values, *i.e.,* the minimum, the nominal and the maximum values of the IC operating temperature. As an example, Figure 3 shows part of the SPICE netlist implementing model (4).

```
* TEMP-DEPENDENT MACROMODEL
.subckt mod w1 w2 ref v
+ PARAMS:
+ Ts = 10e-12
+ Rx = 1
+ T2 = 40 * nominal temperature
+ ...
* output controlled current source i=w1*f1+w2*f2
  Gy ref y1  value={(V(w1)*V(f1)+V(w2)*V(f2))}
  Vy y1  y2  0
  Ry y2  v  {Rx}
* regressors
* dxy11/dt={y-xy11}/Ts
  Rxy11 xy11 0 {Rx}
  Cxy11 xy11 0 {Ts}
  Gxy11 0 xy11 value={V(f1)/Rx}
* dxy21/dt={y-xy21}/Ts
  Rxy21 xy21 0 {Rx}
  Cxy21 xy21 0 {Ts}
  Gxy21 0 xy21 value={V(f2)/Rx}
* dxu1/dt=[v-xu1]/Ts
  Rxu1 xu1 0 {Rx}
  Cxu1 xu1 0 {Ts}
  Gxu1 0 xu1 value={V(v,ref)/Rx}

* f1(T) and f2(T) RBF submodels

  Rf1 f1 0 1
  Ef1 f1 0 value={
  + ((-2.9)+(0.016)*(TEMP-T2)+(-0.06)*abs(TEMP-T2))*EXP(...)+
  + ...
  + )

  Rf2 f2 0 1
  Ef2 f2 0 value={...}

.ends

* w1(T) & w2(T) weight sequencies

  .subckt mod_w1 1 2
   rw 1 2 1
   vw 1 2 PWL(
   + 0 {0.14e-3+(1.77e-6)*(TEMP-T2)+(1.27e-7)*abs(TEMP-T2)}
   + 10e-12 ...
   +)
  .ends

  .subckt mod_w2 1 2
    ...
  .ends
```

Figure 3: Example SPICE netlist

4. Application example

In this Section, we apply the proposed modeling approach to the output port of high-speed drivers used in

IBM mainframe products. The reference responses for the estimation and validation of the sought parametric models are obtained from detailed transistor-level models of the drivers. Such a transistor-level models are actually the virtual device being modeled.

As outlined in Section 3, we approximate the temperature-dependent parameters of the models by two-pieces linear relations interpolating the exact values at the minimum, nominal and maximum device operating temperatures (the *estimation temperatures* in the following). The model parameters and their temperature-dependent approximations are obtained as follows. Three set of identification signals are recorded while the device is at the three temperature values T_j, $j = 1,2,3$. Submodels $i_n(k;T_2)$, $n = 1,2$ for the nominal temperature value are estimated from the identification signal recorded at T_2, obtaining $\boldsymbol{\alpha}_2$, the centers and the spreading parameters for the temperature value T_2. The centers and spreading parameters defining these submodels are used to estimate the linear parameters $\boldsymbol{\alpha}_j$ of submodels $i_n(k,T_j)$, $j = 1,3$ from the identification signal recorded at T_1 and T_3, respectively. Then $\bar{\boldsymbol{\alpha}}(T)$ of (5) is obtained by interpolating $\boldsymbol{\alpha}_j$, $j = 1,2,3$. Once submodels $i_n(k;T_j)$, $n = 1,2$ and $j = 1,2,3$ are known, the weight coefficients $w_n(k;T_j)$ describing state switchings at T_j are computed, and the weight coefficients for the other temperatures are approximated by two-piece linear relations interpolating $w_n(k;T_j)$. Finally the obtained temperature-dependent parametric model (4) is implemented as a subcircuit of the same SPICE environment used to run the transistor-level model of the driver (PowerSPICE [8]).

Example 1: The first device considered is an IBM CMOS driver with power supply $V_{dd} = 1.8\,V$. For this example, the values of the three estimation temperatures are $T_1 = 10\,°C$ (minimum), $T_2 = 40\,°C$ (nominal) and $T_3 = 80\,°C$ (maximum). Figure 4 shows the identification signals used in this example for the estimation of submodels $i_1(k;T_j)$, $j = 1,2,3$. Such voltage and current transient waveforms are responses of the transistor-level model of the driver and are computed for PowerSPICE. The waveforms are sampled with a sampling pitch $t_s = 10\,\text{ps}$ and processed by the algorithm of [6, 7] to obtain the submodel parameters. For this example, the estimated submodels $i_1(k;T_j)$ and $i_2(k;T_j)$ turn out to be composed of seven Gaussian basis function and to have dynamic order $r = 1$. Figure 5 and Figure 6 show the weight coefficients $w_n(k,T_j)$, $n = 1,2$ and $j = 1,2,3$ describing Low-to-High and a High-to-Low state transitions for the minimum, nominal and maximum temperatures. In this example the two reference loads used to generate the reference switching responses and to compute $w_n(k,T_j)$ are a simple $50\,\Omega$ resistor and the series connection of a $50\,\Omega$ resistor and a V_{dd} battery.

In order to verify the accuracy of the obtained model, its responses are compared to the responses of the original transistor-level model for test loads different from the reference loads. As an example, Figure 8 shows the

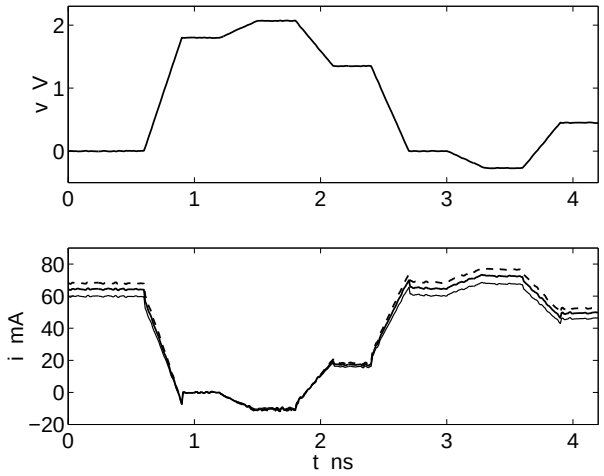

Figure 4: Transient port voltage and current waveforms for the estimation of submodel $i_1(k;T)$ computed at the three different temperatures T_1 (dashed line), T_2 (solid thick line) and T_3 (solid thin line). Top panel: driving voltage waveform applied to the port; bottom panel: port current response.

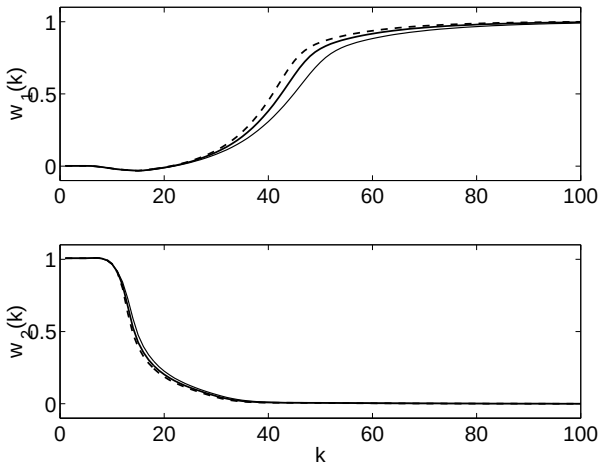

Figure 5: Weight coefficients $w_n(k)$, $n = 1,2$ forcing the model (2) to produce a Low-to-High state transition. Dashed line: $w_n(k)$ estimated for $T = T_1$; solid thick line: $w_n(k)$ estimated for $T = T_2$; solid thin line: $w_n(k)$ estimated for $T = T_3$.

responses of the parametric model and of the reference transistor-level model when they drive a test load composed of an ideal transmission line with characteristic impedance $Z_0 = 50\,\Omega$ and delay $T_d = 40\,\text{ps}$ terminated by a 1 pF capacitor (See Fig. 7). Both the near-end and the far-end voltage waveforms for a single pulse excitation and for $T = 10, 40, 80\,°C$ are shown. This Figure demonstrate the correct operation of the model for a realistic test load and for the temperature values T_j, $j = 1,2,3$ where the exact model parameters are interpolated. Figure 9 repeats the comparison of Fig. 8 at temperature values different from those used for the interpolation of the temperature-dependent model parameters, *i.e.*, $T = -10, 25, 60, 100\,°C$. For all these temper-

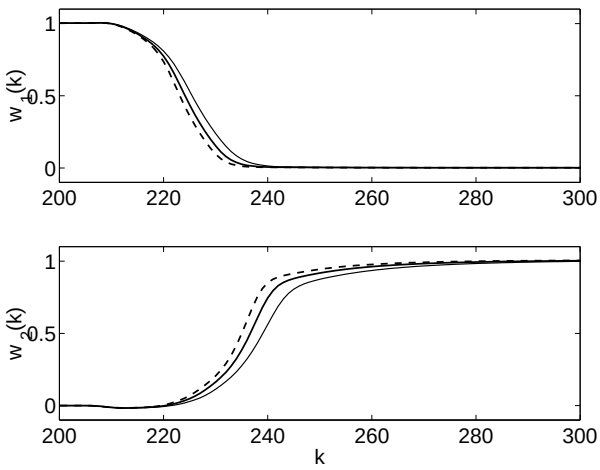

Figure 6: Weight coefficients $w_n(k),\ n = 1, 2$ forcing the model (2) to produce a High-to-Low state transition. Dashed line: $w_n(k)$ estimated for $T = T_1$; solid thick line: $w_n(k)$ estimated for $T = T_2$; solid thin line: $w_n(k)$ estimated for $T = T_3$.

atures, including $T = -10$ and $T = 100$ that are outside the approximation interval $[T_1, T_2]$, the estimated model still reproduces the port reference behavior very well.

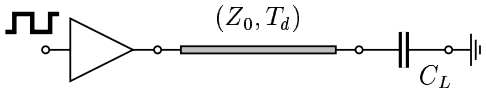

Figure 7: Validation setup. The port being modeled is connected to an ideal transmission line ($Z_0 = 50\,\Omega$, $T_d = 40$ ps) loaded by a 1 pF capacitor.

Example 2: The second device being modeled is a different IBM CMOS driver (power supply $V_{dd} = 2.5$ V) that exhibits a stronger temperature dependence. For this example, the values of the three estimation temperatures are $T_1 = 25\,°C$ (minimum), $T_2 = 55\,°C$ (nominal) and $T_3 = 85\,°C$ (maximum) and the sampling pitch used in the estimation process is $t_s = 10$ ps. In this case, the estimated submodels $i_1(k; T_j)$ and $i_2(k; T_j)$ turn out to be composed of twelve Gaussian basis function and to have dynamic order $r = 2$.

As in the previous example the accuracy of the estimated model has been verified by comparing the model responses to the reference ones for different test loads. Figures 10 and 11 show the result of such comparison for the test load of Fig. 7. Also for this case, the accuracy of the proposed model can be clearly appreciated.

As a conclusion, the accuracy of the proposed temperature-dependent parametric model is comparable to the accuracy the parametric models estimated for the specific temperature of interest. In fact, in the previous validation curves, the timing errors produced by the model are always less that $5 \div 10$ ps, $t_s = 10$ ps being the sampling time used in the estimation process. Besides, since the temperature-dependent model has the same

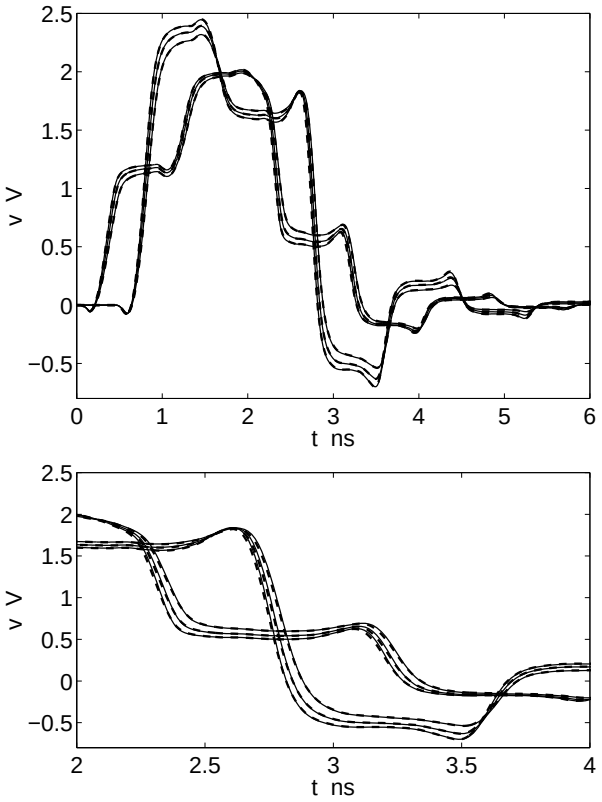

Figure 8: Near-end and far-end voltage waveforms on the transmission line of Fig. 7 for the driver of example #1. The curves are computed for the temperature values $T = 10, 40, 80\,°C$. Solid curves: reference responses; dashed curves: model responses. Top panel: complete waveforms; bottom panel: zoom view.

structure of the parent temperature-independent model, it fully benefits of the simplicity and efficiency of the RBF parametric approach. In terms of figures, this means that the temperature-dependent models can be estimated in some tens seconds by a desktop PC and they are more than tens times faster than the original transistor-level models.

5. Conclusions

We address the development of a temperature-dependent parametric macromodel suitable for the output ports of a digital IC. The parameters defining the model can be readily estimated through a well established procedure from external port transient voltage and current waveforms recorded at a few temperature values. The obtained models are implemented as SPICE subcircuits and turn out to have good accuracy and efficiency levels over a wide temperature range.

Acknowledgements

The authors whish to acknowledge the people of the IBM Enterprise System Group, Poughkeepsie, NY, USA for providing them the reference transistor-level models of the IBM devices and the PowerSPICE simulation tool for computing the curves collected in this paper.

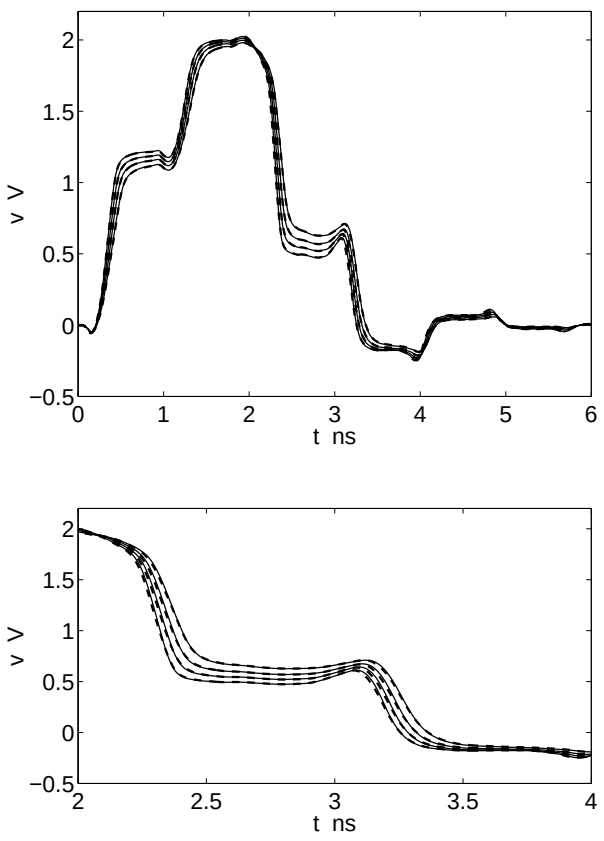

Figure 9: Near-end and far-end voltage waveforms on the transmission line of Fig. 7 for the driver of example #1. The curves are computed for the temperature values $T = -10, 25, 60, 100\,°C$. Solid curves: reference responses; dashed curves: model responses. Top panel: complete waveforms; bottom panel: zoom view.

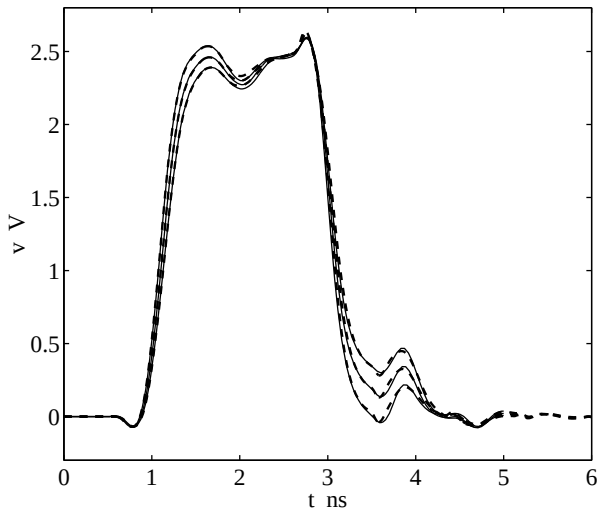

Figure 10: Far-end voltage waveforms on the transmission line of Fig. 7 for the driver of example #2. The curves are computed for the temperature values $T = 25, 55, 85\,°C$. Solid curves: reference responses; dashed curves: model responses.

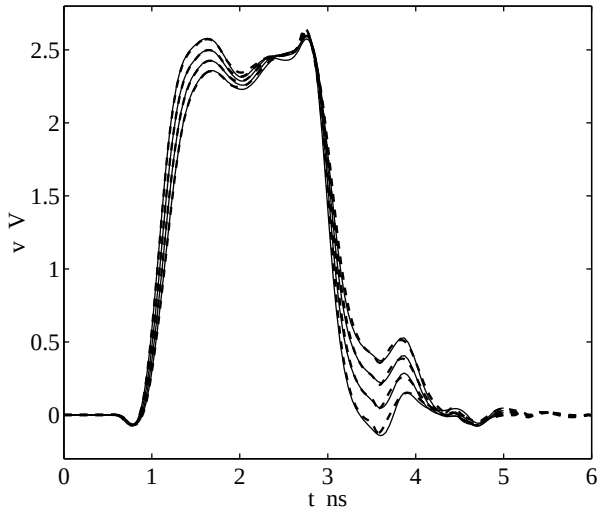

Figure 11: Far-end voltage waveforms on the transmission line of Fig. 7 for the driver of example #2. The curves are computed for the temperature values $T = 10, 40, 70, 100\,°C$. Solid curves: reference responses; dashed curves: model responses.

References

[1] "I/O Buffer Information Specification (IBIS) Ver. 3.2," on the web at `http://-www.eigroup.org/ibis/ibis.htm`, Sep. 1999.

[2] L. Ljung, System Identification: theory for the user. Prentice-Hall, 1987.

[3] I. S. Stievano, F. G. Canavero, I. A. Maio, "Parametric Macromodels of Digital I/O Ports", *IEEE Transactions on Advanced Packaging*, Vol. 25, No. 2, May 2002.

[4] I. S. Stievano, I. A. Maio, "Behavioral models of digital IC ports from measured transient waveforms," *Proc. of the 9^{th} IEEE Topical Meeting on Electrical Performance of Electronic Packaging, EPEP*, Scottsdale, AZ, pp. 211–214, Oct. 23–25, 2000.

[5] J. Sjöberg et al., "Nonlinear Black-Box Modeling in System Identification: a Unified Overview," *Automatica*, Vol. 31, NO. 12, pp. 1691–1724, 1995.

[6] S. Chen, C. F. N. Cowan and P. M. Grant, "Ortogonal Least Squares Learning Algorithm for Radial Basis Function Network," *IEEE Transactions on Neural Networks*, Vol. 2, NO. 2, pp. 302–309, March 1991.

[7] K. Judd and A. Mees, "On selecting models for nonlinear time series," *Physica D*, Vol. 82, pp. 426–444, 1995.

[8] IBM PowerSPICE: User's Guide, Version 1.5, May 31, 2002.